Photoelectron Spectroscopy of Alkoxide and Enolate Negative Ions

G. B. Ellison,* P. C. Engelking,†* and W. C. Lineberger*

Department of Chemistry, University of Colorado, Boulder, Colorado 80309, and Joint Institute for Laboratory Astrophysics, University of Colorado and the National Bureau of Standards, Boulder, Colorado 80309 *(Received: August 9, 1982)*

We report the photoelectron spectra of several alkoxide and enolate negative ions. The spectra are obtained by crossing a mass-selected negative ion beam with the intracavity beam from an Ar II (488 nm) laser and by energy analysis of the resulting photoelectrons. All of the experimental data show at least partially resolved vibrational structure and indicate a substantial geometry change between the neutral radical and the anion. Analysis of the data yields the following electron affinities (in eV): EA(CH_3CH_2O) = 1.726 ± 0.033; EA(CD_3CD_2O) = 1.702 ± 0.033; EA($CH_3CH_2CH_2O$) = 1.789 ± 0.033; EA($(CH_3)_2CHO$) = 1.839 ± 0.029; EA($(CH_3)_3CO$) = $1.912^{+0.029}_{-0.054}$; EA(CH_2CHO) = 1.817 ± 0.023; EA(CD_2CDO) = 1.817 ± 0.029; EA(CH_3CHCHO) = 1.611 ± 0.023; EA($CH_2C(CH_3)O$) = 1.757 ± 0.033.

Introduction

The chemistry and spectroscopy of oxy radicals and ions are being studied by a number of techniques. The gas-phase ion chemistry of alkoxide ions has been studied in ion cyclotron resonance (ICR) spectrometers[1,2] and flowing afterglows.[3-5] A careful review of the ion chemistry has appeared.[6] Several oxy radicals have been characterized by laser-excited fluorescence[7-11] and a detailed analysis of the laser magnetic resonance (LMR) spectrum of CH_3O has been reported.[12,13]

The threshold photodetachment spectra of a large number of enolate and alkoxide ions have been studied by Brauman and co-workers.[14-20] Ions were confined in an ICR trap and the wavelength dependences of their relative photodestruction cross sections were studied with a tunable dye laser. Several enolate ions were scruntinized at high resolution.[17-20] A recent review of all molecular electron affinities has appeared in the series "Gas Phase Ion Chemistry."[21]

We report the photoelectron spectra of several alkoxide and enolate ions. The general process investigated in these experiments is given by eq 1. Electrons with kinetic

$$RO^- + \hbar\omega_0 \rightarrow RO + e^-(KE) \quad (1)$$

energy, KE, are produced by detachment of the negative ions with a fixed-frequency argon ion laser ($\hbar\omega_0$ = 2.540 eV). By energy analysis of the scattered electrons, $e^-(KE)$, we have measured the electron affinities (EA) and several vibronic features of five alkoxide and four enolate ions. This technique was employed earlier[22] to examine CH_3O^- and CH_3S^-.

Experimental Section

Descriptions of negative ion photoelectron spectroscopy apparatus and methods have been presented.[23-25] A sketch of our procedure follows. Negative ions are extracted from a magnetically confined, high-pressure (roughly 0.1 torr) plasma and are formed into a mass-selected beam. This beam collides with an intense, CW laser beam at the inlet of a hemispherical electron energy analyzer. Detached electrons passing through the analyzer are counted and the spectrum of electron counts vs. kinetic energy is formed. The argon ion laser used in these experiments operates on a single line (λ_0 = 488 nm) and the ion beam–laser interaction region is intracavity. Typical intracavity laser powers are about 100 W of circulating power. Electron binding energies are given by the differences between the photon energy and the measured electron kinetic energy, as discussed below.

Ions are produced by admitting the pure alcohol (CH_3CH_2OH, $CH_3CH_2CH_2OH$, $(CH_3)_2CHOH$, and $(CH_3)_3COH$) to the ion source through a controlled leak valve. We have found that thoria-coated iridium filaments routinely provide intense beams of alkoxide and enolate ions. Ion beam currents of 1–5 nA are commonly produced.

The electron analyzer energy scale was calibrated[26] by

† Present address: Department of Chemistry, University of Oregon, Eugene, OR 97403.

(1) R. T. McIver, Jr., and J. S. Miller, *J. Am. Chem. Soc.*, **96**, 4323 (1974).
(2) J. E. Bartmess and R. T. McIver, Jr., *J. Am. Chem. Soc.*, **99**, 4163 (1977).
(3) G. I. Mackay, J. D. Payzant, R. S. Hemsworth, H. I. Schiff, and D. K. Bohme, presented at the 22nd Annual Conference on Mass Spectrometry and Allied Topics, Philadelphia, PA, May 19–24, 1974.
(4) V. M. Bierbaum, C. H. DePuy, R. H. Shapiro, and J. H. Stewart, *J. Am. Chem. Soc.*, **98**, 4229 (1976).
(5) C. H. DePuy and V. M. Bierbaum, *Acc. Chem. Res.*, **14**, 146 (1981).
(6) J. E. Bartmess and R. T. McIver, Jr., in "Gas Phase Ion Chemistry", Vol. 2, M. T. Bowers, Ed., Academic Press, New York, 1979, pp 87–121.
(7) G. Inoue, H. Akimoto, and M. Okuda, *Chem. Phys. Lett.*, **63**, 213 (1979).
(8) G. Inoue, H. Akimoto, and M. Okuda, *J. Chem. Phys.*, **72**, 1769 (1980).
(9) G. Inoue and H. Akimoto, *J. Chem. Phys.*, **74**, 425 (1981).
(10) G. Inoue, M. Okuda, and H. Akimoto, *J. Chem. Phys.*, **75**, 2060 (1981).
(11) D. E. Powers, J. B. Hopkins, and R. E. Smalley, *J. Phys. Chem.*, **85**, 2711 (1981).
(12) H. E. Radford and D. K. Russell, *J. Chem. Phys.*, **66**, 2222 (1977).
(13) D. K. Russell and H. E. Radford, *J. Chem. Phys.*, **72**, 2750 (1980).
(14) A. H. Zimmerman, K. J. Reed, and J. I. Brauman, *J. Am. Chem. Soc..*, **99**, 7203 (1977).
(15) A. H. Zimmerman, R. L. Jackson, B. K. Janousek, and J. I. Brauman, *J. Am. Chem. Soc.*, **100**, 4674 (1978).
(16) B. K. Janousek, A. H. Zimmerman, K. J. Reed, and J. I. Brauman, *J. Am. Chem. Soc.*, **100**, 6142 (1978).
(17) A. H. Zimmerman and J. I. Brauman, *J. Chem. Phys.*, **66**, 5823 (1977).
(18) R. L. Jackson, A. H. Zimmermann, and J. I. Brauman, *J. Chem. Phys.*, **71**, 2088 (1979).
(19) R. W. Wetmore, H. F. Schaefer, III, P. C. Hiberty, and J. I. Brauman, *J. Am. Chem. Soc.*, **102**, 5470 (1980).
(20) R. L. Jackson, P. C. Hiberty, and J. I. Brauman, *J. Chem. Phys.*, **74**, 3705 (1981).
(21) B. K. Janousek, and J. I. Brauman in "Gas Phase Ion Chemistry", Vol. 2, M. T. Bowers, Ed., Academic Press, New York, 1979, pp 53–86.
(22) P. C. Engleking, G. B. Ellison, and W. C. Lineberger, *J. Chem. Phys.*, **69**, 1826 (1978).
(23) M. W. Siegel, R. J. Celotta, J. L. Hall, J. Levine, and R. A. Bennett, *Phys. Rev. A*, **6**, 607 (1972).
(24) R. J. Celotta, R. A. Bennett, J. L. Hall, M. W. Siegel, and J. Levine, *Phys. Rev. A*, **6**, 631 (1972).
(25) P. C. Engelking, R. R. Corderman, J. J. Wendoloski, G. B. Ellison, S. V. ONeil, and W. C. Lineberger, *J. Chem. Phys.*, **74**, 5460 (1981).
(26) P. C. Engelking and W. C. Lineberger, *J. Chem. Phys.*, **65**, 4323 (1976).

0022-3654/82/2086-4873$01.25/0

TABLE I: Photoelectron Peak Positions and Splittings

peak	kinetic energy, eV	splitting, cm^{-1}
	$CH_3CH_2O^-$	
0, 0	0.814	
A	0.680	1100 ± 150
B	0.541	1100 ± 150
C	0.401	1100 ± 250
D	0.262	1100 ± 300
	$CD_3CD_2O^-$	
0, 0	0.831	
A	0.728	850 ± 200
B	0.604	1000 ± 250
C	0.486	950 ± 300
D	0.367	950 ± 300
	$CH_3CH_2CH_2O^-$	
0, 0	0.751	
A	0.627	1000 ± 250
B	0.467	1300 ± 300
C	0.302	1300 ± 300
	$(CH_3)_2CHO^-$	
0, 0	0.701	
A	0.649	400 ± 150
B	0.557	750 ± 150
C	0.500	450 ± 150
D	0.412	700 ± 250
E	0.319	750 ± 300
F	0.289	250 ± 300
	$(CH_3)_3CO^-$	
0, 0	0.628	
A	0.592	300 ± 200
B	0.489	800 ± 300
	$CH_2=CHO^-$	
0, 0	0.723	
A	0.666	450 ± 50
B	0.599	550 ± 150
C	0.537	500 ± 150
D	0.476	500 ± 250
E	0.409	550 ± 250
	$CD_2=CDO^-$	
0, 0	0.723	
A	0.677	350 ± 150
B	0.620	450 ± 150
C	0.563	450 ± 150
D	0.506	450 ± 150
E	0.445	500 ± 200
	$CH_3CH=CHO^-$	
0, 0	0.929	
A	0.852	600 ± 150
B	0.764	700 ± 100
C	0.687	600 ± 150
D	0.594	750 ± 200
E	0.424	1350 ± 300
	$CH_2=C(CH_3)-O^-$	
A	0.922	
0, 0	0.783	1100 ± 150
B	0.716	550 ± 150
C	0.654	500 ± 150
D	0.587	550 ± 150
E	0.515	600 ± 200

detaching NH^- and examining the splitting between NH($^3\Sigma^-$) and NH($^1\Delta$). This energy gap has been independently established by optical spectroscopy[27] and thus serves to calibrate our hemispherical energy analyzer. The absolute energy scale is fixed by detaching a reference ion; in this case we have used O^-. The "effective" EA of O is known[28] to be 1.465 ± 0.005 eV. Electron spectra reported in this paper are plots of total electron counts vs. the center of mass kinetic energy (KE) of the photoelectrons. The working expression[22] for the center of mass KE of electrons detached from an ion of mass M with beam energy W is

$$\mathrm{KE} = 2.540 - 1.465 - \gamma[T(O^-) - T(M^-)] - mW[1/16 - 1/M] \quad (2)$$

In this expression, T is the observed laboratory frame kinetic energy of electrons from M^- and O^-, respectively. The constant γ is a scale compression correction factor determined as above from NH^- photodetachment.[26] The argon ion laser is employed at λ_0 = 488 nm (2.540 eV) and m is the mass of the electron. The hemispherical analyzer has an energy resolution of about 60 meV (fwhm). Under favorable conditions it is possible to determine absolute electron binding energies to an accuracy of 10 meV.

The intensity of photoelectrons at a given energy depends on the angle, θ, between the electric vector of the light and the electron collection direction.[29,30] We have set θ = 54.7° to ensure that the measured cross section was proportional to the total cross section.

TABLE II: Final Experimental Electron Affinities (EA)[a]

neutral	final EA	lit.	ref
CH_3CH_2-O	1.726 ± 0.033	1.52 ± 0.12	3
CD_3CD_2-O	1.702 ± 0.033		
$CH_3CH_2CH_2-O$	1.789 ± 0.033		
$(CH_3)_2CH-O$	1.839 ± 0.029	1.54 ± 0.18	3
$(CH_3)_3C-O$	$1.912^{+0.029}_{-0.054}$	1.87 ± 0.01 or	15
		1.90 ± 0.01	15
$CH_2=CH-O$	1.817 ± 0.023	1.824 ± 0.005	20
$CD_2=CD-O$	1.817 ± 0.029	1.819 ± 0.005	20
$CH_3CH=CH-O$	1.611 ± 0.023	1.687 ± 0.052	14
$CH_2=C(CH_3)-O$	1.757 ± 0.033	1.761 ± 0.056	14

[a] All values in electron volts.

Results and Discussion

The photoelectron spectra of the alkoxide ions are shown in Figures 1–5 and the enolate spectra continue from Figure 6 through Figure 9. The electron affinities are simply the differences between the laser photon energy (2.540 eV) and the KE of the electrons assigned to the [(ion)v'' = 0] → [(neutral)v' = 0] transition. Table I collects the line positions for all of the vibronic features marked in Figures 1–9.

Table II lists the final electron affinities together with errors stemming from various corrections. The proper EA is the energy between the lowest ro-vibronic level of the lowest spin–orbit component of the ion and the corresponding state of the neutral. Strategies for estimating the rotational, vibrational, and spin–orbit corrections are sketched in ref 22 for CH_3O and CH_3S. For the asymmetric alkoxide and enolate ions discussed here, little is known of the rotational constants or vibrational frequencies and as a result most of these corrections and the corresponding errors only can be estimated. The contribution to our final error bars from each of these factors is as follows: rotational correction ±0.005 eV, vibrational sequence band correction ±0.020 eV, and the spin–orbit correction ±0.005 eV. The couplings of spin to other angular momenta are considered negligible for this experiment.

If the gas-phase acidity, $\Delta H°_{acid}$, and the neutral heat of formation, $\Delta H_f°_{298}$, are known, then determination of the EA enables the calculation of several important thermodynamic properties.[6] With the data listed in Table

(27) C. Zetzsch and F. Stuhl, *Chem. Phys. Lett.*, **33**, 375 (1975).
(28) H. Hotop and W. C. Lineberger, *J. Phys. Chem. Ref. Data*, 4, 539 (1975).
(29) J. Cooper and R. N. Zare, *J. Chem. Phys.*, **48**, 942 (1968).
(30) J. L. Hall and M. W. Siegel, *J. Chem. Phys.*, **48**, 943 (1968).

TABLE III: Thermodynamic Properties of Alcohols[a]

ROH	$\Delta H_f^\circ{}_{298}$(ROH)	ΔH°_{acid}(ROH)	EA(RO)	DH°(RO-H)	$\Delta H_f^\circ{}_{298}$(RO)	$\Delta H_f^\circ{}_{298}$(RO^-)
HO-H	−57.796	390.8 ± 0.4	42.1471 ± 0.0005	119.4 ± 0.5	9.5 ± 0.5	−32.7 ± 0.6
CH_3O-H	−47.96	379.2 ± 2	36.2 ± 0.5	102 ± 2	2 ± 2	−34 ± 2
CH_3CH_2O-H	−56.19	376.1 ± 2	39.8 ± 0.8	102 ± 2	−6 ± 2	−46 ± 2
$CH_3(CH_2)_2O$-H	−61.55	374.7 ± 2	41.3 ± 0.8	102 ± 2	−12 ± 2	−53 ± 2
$(CH_3)_2CHO$-H	−65.15	374.1 ± 2	42.4 ± 0.7	103 ± 2	−14 ± 2	−56 ± 2
$(CH_3)_3CO$-H	−77.87	373.3 ± 2	44.1 ± 1.2	104 ± 2	−26 ± 2	−70 ± 2

[a] All values are in kcal mol^{-1}. The values of $\Delta H_f^\circ{}_{298}$(ROH) are from Table 7.2 of ref 31. The values of ΔH°_{acid}(ROH) are from Table III of ref 6. The EA(OH) is from ref 40 and the EA(CH_3O) is from ref 22. All other electron affinities are from this paper, Table II.

TABLE IV: Thermodynamic Properties of Acetaldehyde, Propionaldehyde, and Acetone[a]

RH	$\Delta H_f^\circ{}_{298}$(RH)	ΔH°_{acid}(RH)	EA(R)	DH°(R-H)	$\Delta H_f^\circ{}_{298}$(R)	$\Delta H_f^\circ{}_{298}$(R^-)
H-CH_2CHO	−39.72	366.4 ± 2	41.9 ± 0.5	95 ± 2	3 ± 2	−39 ± 2
H-$CH(CH_3)CHO$	−45.90	365.9 ± 2	37.2 ± 0.5	90 ± 2	−8 ± 2	−45 ± 2
H-CH_2COCH_3	−52.00	368.8 ± 2	40.5 ± 0.8	96 ± 2	−8 ± 2	−49 ± 2

[a] All values are in kcal mol^{-1}. The values of $\Delta H_f^\circ{}_{298}$(RH) are from Table 7.2 of ref 31. The values of ΔH°_{acid}(RH) are from Table III of ref 6. All electron affinities are from this paper, Table II.

II, the gas-phase acidities can yield bond dissociation energies, DH°.

$$\Delta H^\circ_{acid}(RO\text{–}H) \cong DH^\circ(RO\text{–}H) - EA(RO) + IP(H) \quad (3)$$

The ionization potential (IP) of hydrogen is 313.6 kcal mol^{-1} while its heat of formation is 52.1 kcal mol^{-1}. once the bond dissociation energy is established, the $\Delta H_f^\circ{}_{298}$(RO) can be calculated. Finally, $\Delta H_f^\circ{}_{298}$(RO) and the

$$DH^\circ(RO\text{–}H) = \Delta H_f^\circ{}_{298}(RO) + \Delta H_f^\circ{}_{298}(H) - \Delta H_f^\circ{}_{298}(ROH) \quad (4)$$

EA(RO) combine to afford the heat of formation of the negative ion, RO^-.

$$\Delta H_f^\circ{}_{298}(RO^-) = \Delta H_f^\circ{}_{298}(RO) - EA(RO) \quad (5)$$

All of these thermodynamic properties are presented in Tables III and IV. A discussion of several individual ions now follows.

Ethoxide. The photoelectron spectrum of $CH_3CH_2O^-$ is shown in Figure 1 while $CD_3CD_2O^-$ occupies Figure 2. The spectrum in Figure 1 results from detachment of the m/z 45 ion beam produced by ethanol. If CD_3CD_2OH is used instead of ethanol, and the m/z 50 ion beam is selected, the spectrum obtained is the one shown in Figure 2. The origin in each spectrum is labeled (0,0) and directly yields the corresponding electron affinities: EA(CH_3CH_2O) = 1.726 ± 0.033 eV and EA(CD_3CD_2O) = 1.702 ± 0.033 eV. The vibronic features characterizing ethoxide ion detachment are not simple. Each of the features in Figure 1 ((0,0), A, B, C, and D) is surely a composite of a number of blended lines, indicating that more than one vibrational mode is excited in the photodetachment process. The scale expansion in Figures 1 and 2 (magnified by a factor of 5) reveals a feature that we attribute to detachment from vibrationally excited ethoxide ions ("hot bands"). The kinetic energy at which these hot bands appear is at about 0.97 eV (for $C_2H_5O^-$) and roughly 0.98 eV (for $C_2D_5O^-$). This places the vibrational frequency excited in $C_2H_5O^-$ at 1250 ± 400 cm^{-1} while that for $C_2D_5O^-$ is 1200 ± 400 cm^{-1}.

Both the microwave[32] and infrared[33] spectroscopies of

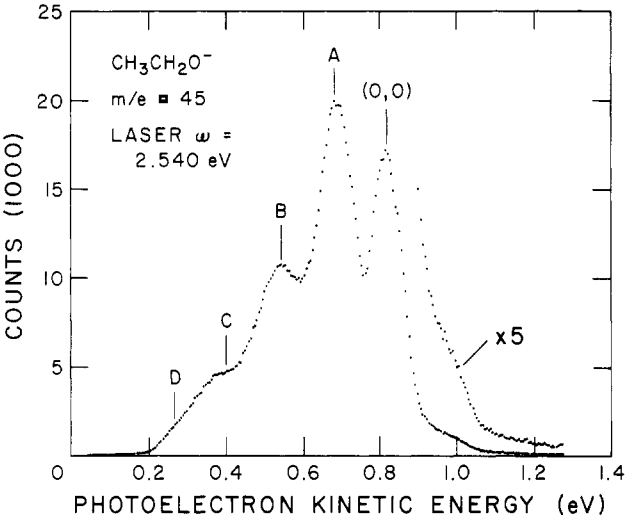

Figure 1. Photoelectron spectrum obtained from a beam of ethoxide ion, $CH_3CH_2O^-$. Each data point is roughly 5 meV wide.

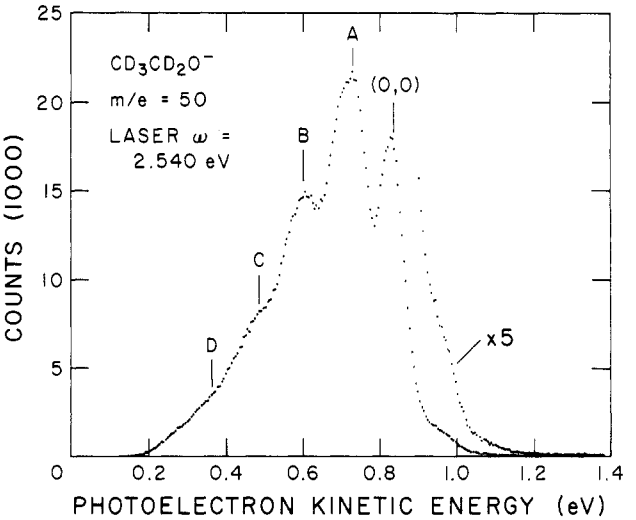

Figure 2. Photoelectron spectrum obtained from a beam of deuterated ethoxide ion, $CD_3CD_2O^-$. Each data point is approximately 5 meV wide.

CH_3CH_2OH have been reported. Our slight knowledge of the ethoxy radical (CH_3CH_2O) is summarized by Inoue, Okuda, and Akimoto.[10] While the symmetries of both the $\tilde{X}$ and $\tilde{A}$ states of ethoxyl are not experimentally estab-

(31) H. M. Rosenstock, K. Draxl, B. W. Steiner, and J. T. Herron, *J. Phys. Chem. Ref. Data*, **6**, supplement no. 1 (1977).
(32) M. Takano, Y. Sasada, and T. Satoh, *J. Mol. Spectrosc.*, **26**, 157 (1968).
(33) A. J. Barnes, and H. E. Haller, *Trans. Faraday Soc.*, **66**, 1932 (1970).
(34) R. J. Cvetanovic, *Adv. Photochem.*, **1**, 115 (1963).
(35) J. R. Kanofsky and D. J. Gutman, *Chem. Phys. Lett.*, **15**, 236 (1972).

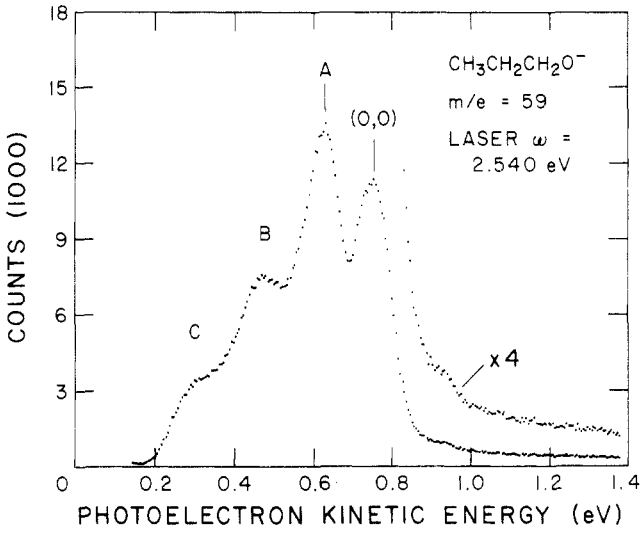

Figure 3. Photoelectron spectrum obtained from a beam of *n*-propyl oxide ion, $CH_3CH_2CH_2O^-$. Each data point is roughly 5 meV wide.

lished, the ground, $\tilde{X}$ state of ethoxide ion is surely $^1A'$. We can thus represent the detachment process follows:

$$CH_3CH_2O^- \; \tilde{X}(^1A') + h\nu_0 \begin{cases} \rightarrow CH_3CH_2O \; \tilde{X}_2(^2A'') \\ \rightarrow CH_3CH_2O \; \tilde{X}_1(^2A') \end{cases} \quad (6)$$

The two states, $\tilde{X}_1$ and $\tilde{X}_2$, result from detachment of the in-plane or out-of-plane "p-like" electrons. The resultant states can be considered as almost degenerate components of one $\tilde{X}$ state. The energy splitting is unknown, but the photoelectron spectrum indicates that it must be about 1000 cm^{-1} or less, otherwise the spectrum would show evidence of doubling. An $\tilde{A} \rightarrow \tilde{X}$ transition has been studied by laser-excited fluorescence[10] and $\Delta E(\tilde{A}-\tilde{X})$ = 29204 cm^{-1} (3.621 eV). Vibrational modes identified in $\tilde{X}(CH_3CH_2O)$ were ω_5 = 1367 cm^{-1} (CH_2 wagging mode), ω_9 = 1073 cm^{-1} (out-of-phase C–C–O stretch), ω_{10} = 873 cm^{-1} (in-phase C–C–O stretch), and ω_{11} = 442 cm^{-1} (C–C–O bend). The out-of-phase C–C–O stretch (ω_9) is known to be quite harmonic.[10] It is tempting to consider the progression ((0,0), A, B, C, and D) in both Figures 1 and 2 as involving a series in ω_9 in ethoxyl. With the photoelectron spectra at hand, this can only be a conjecture.

Other Alkoxides. Electron spectra of the higher alkoxides are displayed in Figures 3–5. While vibronic structure is clearly resolved, it is not possible to make any conclusive assignments for the labeled vibronic features. There seem to be a number of active modes but very little is known of the spectroscopy or molecular constants of the corresponding alkoxy radicals. This lack of assignment, however, does not impede the determination of electron affinities. The spectrum of the *tert*-butoxide ion (Figure 5) is particularly dense and featureless; our data are consistent with but do not improve on the earlier determination[15] of the EA($(CH_3)_3O$).

Vinyl Oxide. The acetaldehyde enolate or vinyl oxide ion, $CH_2{=}CH{-}O^-$, has been studied by Brauman and co-workers.[14,15] The vinyloxy radical, CH_2CHO is an intermediate of great interest.[36-38] This species is believed to be the primary product formed from the oxidation of ethylene by $O(^3P)$. The oxidation of olefins has been

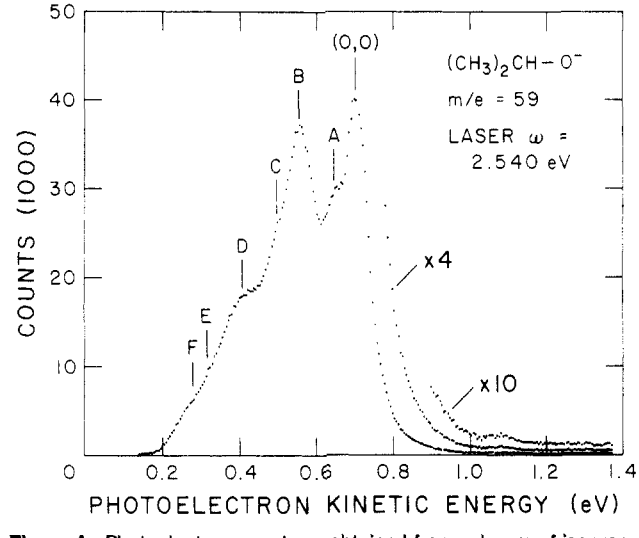

Figure 4. Photoelectron spectrum obtained from a beam of isopropyl oxide ion, $(CH_3)_2CHO^-$. Each data point is approximately 5 meV wide.

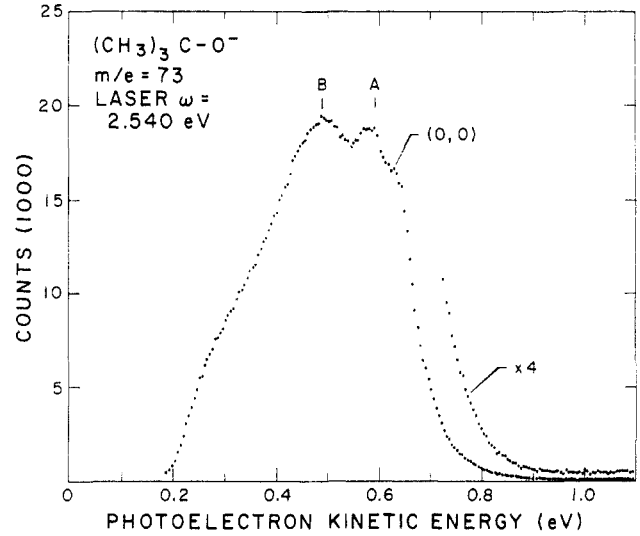

Figure 5. Photoelectron spectrum obtained from a beam of *tert*-butoxide ion, $(CH_3)_3CO^-$. Each data point is roughly 5 meV wide.

studied by a large number of laboratories.[34-38] Laser-excited fluorescence spectroscopy[9,38] and absorption spectroscopy[37] have identified the $\tilde{A}$ and $\tilde{B}$ states of CH_2CHO. Inoue and Akimoto[9] have assigned three vibrational modes of the $\tilde{X}$ state of CH_2CHO. These are called ω_1 = 1560 cm^{-1} (C–O stretch), ω_2 = 1150 cm^{-1} (C–C stretch), and ω_3 = 530 cm^{-1} (C–C–O bend).

The $\tilde{X}$ state of vinyl oxide ion is certainly $^1A'$. Dupuis, Wendoloski, and Lester[39] have completed a computational study of the vinyloxy radical in which they use MCHF techniques, and are able to assign the lowest three electronic states of CH_2CHO as $\tilde{X}$ = $^2A''$, $\tilde{A}$ = $^2A'$, and $\tilde{B}$ = $^2A''$. Their computed splittings among these three states are in excellent agreement with those found experimentally:[9,37,38] $\Delta E(\tilde{X}-\tilde{A})$ = 0.99 eV and $\Delta E(\tilde{X}-\tilde{B})$ = 3.57 eV. We can consider detachment of $CH_2{=}CH{-}O^-$ with eq 7.

$$CH_2{=}CH{-}O^- \; \tilde{X}(^1A') + h\nu_0 \begin{cases} \rightarrow CH_2CHO \; \tilde{B}(^2A'') \\ \rightarrow CH_2CHO \; \tilde{A}(^2A') \\ \rightarrow CH_2CHO \; \tilde{X}(^2A'') \end{cases} \quad (7)$$

(36) R. J. Buss, R. J. Baseman, G. He, and Y. T. Lee, *J. Photochem.*, 17, 389 (1981).
(37) H. E. Hunziker, H. Kneppe, and H. R. Wendt, *J. Photochem.*, 17, 377 (1981).
(38) K. Kleinermanns and A. C. Luntz, *J. Phys. Chem.*, 85, 1966 (1981).
(39) M. Dupuis, J. J. Wendoloski, and W. A. Lester, Jr., *J. Chem. Phys.*, 76, 488 (1982).
(40) P. A. Schulz, R. D. Mead, P. L. Jones, and W. C. Lineberger, *J. Chem. Phys.*, in press.

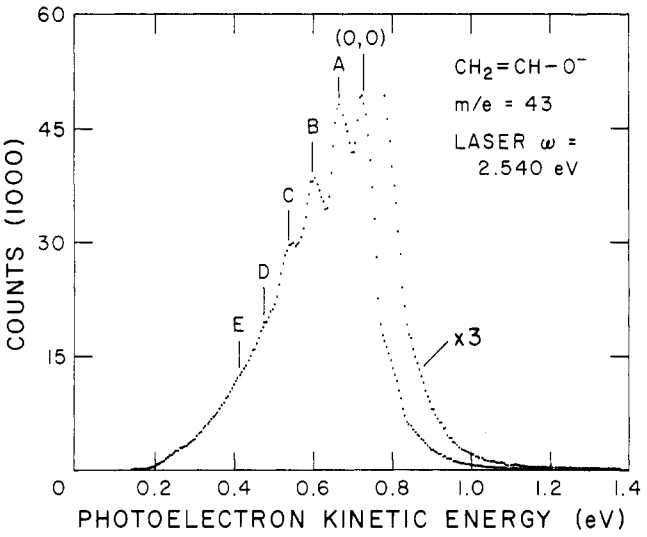

Figure 6. Photoelectron spectrum obtained from a beam of vinyl oxide ion, CH_2=CHO$^-$. Each data point is approximately 5 meV wide.

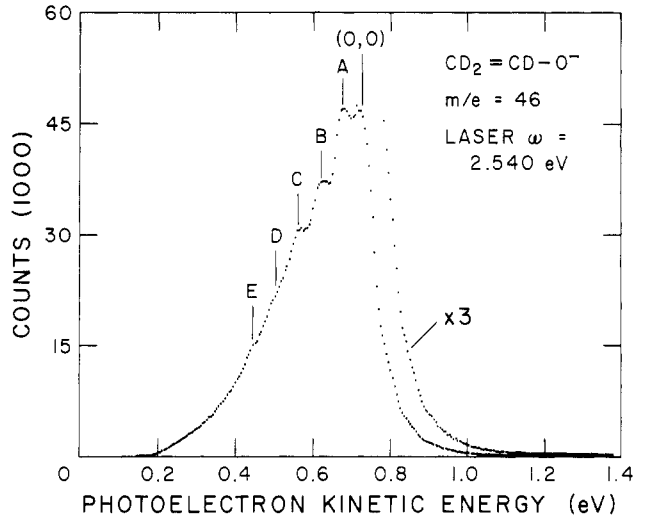

Figure 7. Photoelectron spectrum obtained from a beam of deuterated vinyl oxide ion, CD_2CDO^-. Each data point is roughly 5 meV wide.

If our laser is energetic enough, we expect to observe production of the $\tilde{X}$, $\tilde{A}$, and $\tilde{B}$ states of CH_2CHO. The photoelectron spectra in Figure 6 and 7, together with the known 1-eV excitation spectrum of the lowest excited state, indicate that our argon ion laser can only access the $\tilde{X}$ state of CH_2CHO. It is important to notice that our EA(C_2H_3O) is 1.817 eV—identical with the value that Brauman reported earlier[14,15] (see Table III). The acetaldehyde enolate studied in the ICR was produced by the reaction of F^- with CH_3CHO, while the m/z 43 data in Figure 6 result from adding ethanol to an electric discharge ion source. Since the ions produced in these two different sources possess the same EA, we assert that they are the same species. Consequently we write the m/z 43 ion produced from ethanol as CH_2=CH—O^- and not as the vinyl ion, HC=CH(OH)$^-$. The extent of vibronic structure in the spectrum shows that the geometry of the ion is changed from that of the $\tilde{X}$ state of vinyloxy radical (estimated in ref 39). The vibronic features labeled in Figures 6 and 7 are complex. It is inviting to speculate that ω_3 is one of the modes excited upon detachment. Certainly the intervals tabulated in Table I for $C_2H_3O^-$ and $C_2D_3O^-$ are consistent with such a notion.

Other Enolates. The photoelectron spectra for propionaldehyde enolate and acetone enolate are shown in Figures 8 and 9. These ions are produced by adding

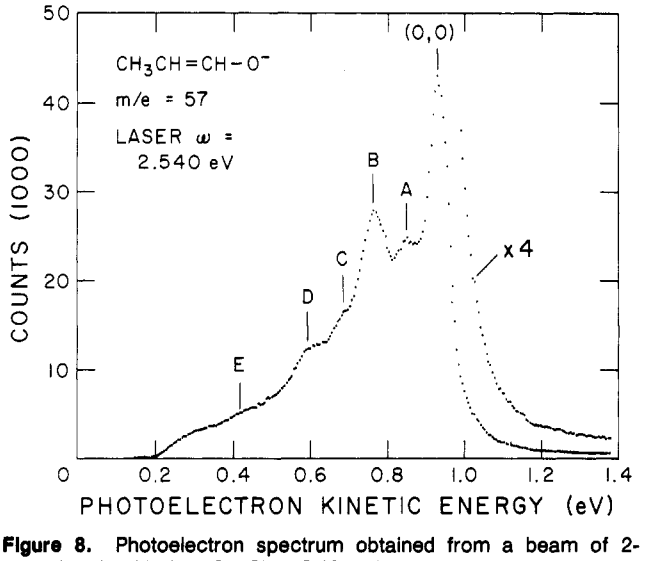

Figure 8. Photoelectron spectrum obtained from a beam of 2-methylvinyl oxide ion, CH_3CH=CHO$^-$. Each data point is roughly 5 meV wide.

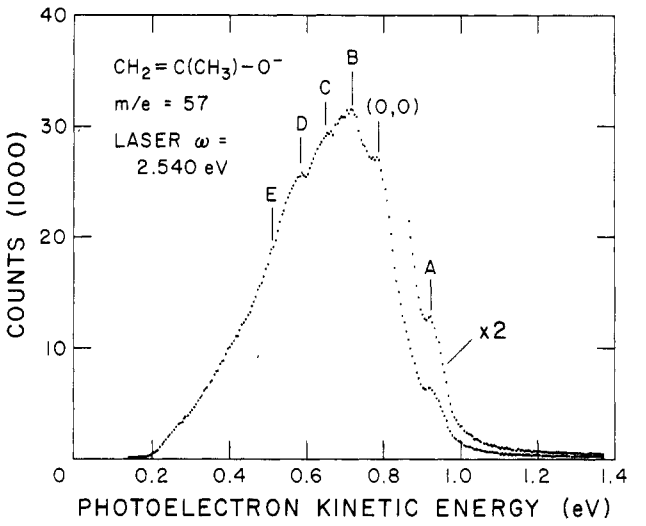

Figure 9. Photoelectron spectrum obtained from a beam of 1-methylvinyl oxide ion, CH_2=C(CH_3)O$^-$. Each data point is roughly 5 meV wide.

1-propanol or 2-propanol to our ion source. The basis for ion identification again rests on a comparison of our electron affinities with the earlier threshold spectra. Table II indicates that the electron affinities of these m/z 57 ions are identical with the values reported by Zimmerman et al.[14] for propionaldehyde enolate and acetone enolate. In this case the ions were produced by F^- proton abstraction reactions. The vibronic structure of these isomeric ions is not readily interpreted. The feature labeled A in Figure 9 is certainly a hot band. Its intensity relative to the (0,0) peak changes substantially depending upon the conditions in our ion source.

Conclusion

All of the photoelectron spectra presented in this paper indicate that a substantial geometry change occurs on going from the neutral radical to the negative ion. The basis for our ion identification is the use of mass-selected ion beams and comparison with Brauman's earlier threshold spectra. Extraction of the EA from these spectra is straightforward, albeit complicated by hot bands in some cases. Examination of these ions with a spectrometer having higher resolution and synthesis of these enolate and alkoxide ions from suitably deuterated precursors could

be expected to extend our understanding of these ionic structures.

Acknowledgment. G.B.E. and P.C.E. thank the A. P. Sloan Foundation for Fellowships. W.C.L. holds a J. S. Guggenheim Memorial Fellowship and a University of Colorado Faculty Fellowship. This work was supported by the National Science Foundation through grants PHY79-04928 and CHE78-18424 to the University of Colorado.

Ab Initio Molecular Orbital Studies of H + C_2H_4 and F + C_2H_4. 1. Comparison of the Equilibrium Geometries, Transition Structures, and Vibrational Frequencies

H. Bernhard Schlegel[†]

Department of Chemistry, Wayne State University, Detroit, Michigan 48202 *(Received: April 23, 1982)*

For the reactions H + $C_2H_4 \rightleftarrows C_2H_5$ and F + $C_2H_4 \rightarrow C_2H_4F \rightarrow$ H + C_2H_3F, the equilibrium geometries and transition structures were fully optimized at the HF/3-21G, HF/6-31G*, and MP2/3-21G levels. Vibrational frequencies were computed for each structure at the HF/3-21G level. While basis set and correlation effects cause large changes in the energy differences, only small and predictable variations are found in the geometries. The β-fluoroethyl radical adopts a gauche conformation in agreement with ESR measurements and matrix isolation IR spectra. The three transition structures are quite similar with the attacking (or leaving) atom ca. 2 Å from the carbon and making an angle of ca. 105° with the CC double bond. The ethylenic moiety is only slightly distorted in the transition state. The bending frequencies for the attacking (or leaving) atom are somewhat higher than previous estimates: 242 and 405 cm^{-1} for F + C_2H_4, 415 and 448 cm^{-1} for H + C_2H_4, 461 and 552 cm^{-1} for H + C_2H_3F.

Introduction

The gas-phase reactions of ethylene with atoms such as hydrogen, fluorine, chlorine, etc. have received considerable attention both experimentally[1-7] and theoretically.[8-21] These reactions proceed in two steps: (i) a bimolecular interaction to form a long-lived complex, ethyl radical, or β-haloethyl radical, and (ii) the unimolecular decomposition of this complex to yield ethylene or vinyl halide plus hydrogen atom. For the reactant and product olefins, experimental structures[22,23] and vibrational frequencies[24,25] are available. The intermediate radicals are less well characterized, with ESR studies in solution[26] and matrix isolation infrared spectra[27,28] providing qualitative information on structure and conformation. The nature of the energy surface connecting the reactants, intermediate radical, and products has been probed by classical chemical kinetics,[2-4] crossed molecular beam techniques,[5,6] and chemiluminescence studies.[7] Theoretical work includes molecular orbital calculations[8-13] as well as statistical kinetics[2-7,14-17] and molecular dynamics studies[12,17-21] of the reaction rates and energy distributions. Computations on the hydrogen plus ethylene system are more numerous and more elaborate than for halogen plus ethylene.

In the present paper, we wish to compare hydrogen and fluorine attacking ethylene. Thus, calculations of similar quality are required for both energy surfaces. Emphasis is placed on the geometry at the minima and the saddle points and the vibrational frequencies of these structures. In particular, the effects of polarization functions and correlation energy on the equilibrium geometries are considered in detail. In a subsequent paper,[29] we undertake the more difficult task of calculating reliable relative energies, approximate barrier heights, and estimated heats of reaction, based on the optimized geometries obtained in the present work.

[†] Fellow of the Alfred P. Sloan Foundation, 1981-3.

(1) W. E. Jones, S. D. MacKnight, and L. Teng, *Chem. Rev.*, **73**, 407 (1973).
(2) J. V. Michael and G. N. Suess, *J. Chem. Phys.*, **58**, 2807 (1973); J. A. Cowfer and J. V. Michael, *ibid.*, **62**, 3504 (1975).
(3) J. H. Lee, J. V. Michael, W. A. Payne, and L. J. Stief, *J. Chem. Phys.*, **68**, 1017 (1978).
(4) K. Sugawara, K. Okazaki, and S. Sato, *Chem. Phys. Lett.*, **78**, 259 (1981).
(5) J. M. Parson and Y. T. Lee, *J. Chem. Phys.*, **56**, 4658 (1972).
(6) J. M. Farrar and Y. T. Lee, *J. Chem. Phys.*, **65**, 1414 (1976).
(7) M. G. Moss, M. D. Ensminger, G. M. Stewart, D. Mordaunt, and J. D. McDonald, *J. Chem. Phys.*, **73**, 1256 (1980), and earlier work.
(8) V. B. Kontecky, K. Kontecky, and L. Salem, *J. Am. Chem. Soc.*, **99**, 842 (1977).
(9) C. S. Sloane and W. L. Hase, *Discuss. Faraday Soc.*, **62**, 210 (1977); W. L. Hase, G. Mrowka, R. J. Brudzynski, and C. S. Sloane, *J. Chem. Phys.*, **69**, 3548 (1978).
(10) D. T. Clark, I. W. Scanlan, and J. C. Walton, *Chem. Phys. Lett.*, **55**, 102 (1978).
(11) S. Nagase and C. W. Kern, *J. Am. Chem. Soc.*, **102**, 4513 (1980).
(12) S. Kato and K. Morokuma, *J. Chem. Phys.*, **72**, 206 (1980).
(13) L. B. Harding, *J. Am. Chem. Soc.*, **103**, 7469 (1981).
(14) S. Nagase, T. Fueno, and K. Morokuma, *J. Am. Chem. Soc.*, **101**, 5849 (1979).
(15) R. A. Marcus, *J. Chem. Phys.*, **62**, 1372 (1975); G. Worry and R. A. Marcus, *ibid.*, **67**, 1636 (1977).
(16) M. Quack, *Chem. Phys.*, **51**, 353 (1980).
(17) D. J. Zvijac and L. C. Light, *Chem. Phys.*, **21**, 411 (1977); D. J. Zvijac, S. Mukamel, and J. Ross, *J. Chem. Phys.*, **67**, 2007 (1977).
(18) W. L. Hase, R. J. Wolf, and C. S. Sloane, *J. Chem. Phys.*, **71**, 2911 (1979).
(19) W. L. Hase, D. M. Ludlow, R. J. Wolf, and T. Schlick, *J. Phys. Chem.*, **85**, 958 (1981).
(20) W. L. Hase and K. C. Bhalla, *J. Chem. Phys.*, **75**, 2807 (1981).
(21) W. L. Hase and D. G. Buckowski, *J. Comput. Chem.*, **3**, 335 (1982).
(22) J. L. Duncan, I. J. Wright, and D. van Lerberghe, *J. Mol. Spectrosc.*, **42**, 251 (1972).
(23) D. R. Lide, Jr., and D. Christensen, *Spectrochim. Acta*, 17, 665 (1961).

0022-3654/82/2086-4878$01.25/0